

EDGE ARTICLE

Cite this: *Chem. Sci.*, 2023, 14, 5460

All publication charges for this article have been paid for by the Royal Society of Chemistry

Received 26th January 2023

Accepted 25th April 2023

DOI: 10.1039/d3sc00435j

rsc.li/chemical-science

Electron-rich benzofulvenes as effective dipolarophiles in copper(i)-catalyzed asymmetric 1,3-dipolar cycloaddition of azomethine ylides†

Xin Chang,^{‡ab} Xue-Tao Liu,^{‡ab} Fangfang Li,^{‡c} Yuhong Yang,^c Lung Wa Chung^{id}*^c and Chun-Jiang Wang^{id}*^{ab}

A series of benzofulvenes without any electron-withdrawing substituents were employed as 2π -type dipolarophiles for the first time to participate in Cu(I)-catalyzed asymmetric 1,3-dipolar cycloaddition (1,3-DC) reactions of azomethine ylides. An intrinsic non-benzenoid aromatic characteristic from benzofulvenes serves as a key driving force for activation of the electron-rich benzofulvenes. Utilizing the current methodology, a wide range of multi-substituted chiral spiro-pyrrolidine derivatives containing two contiguous all-carbon quaternary centers were formed in good yield with exclusive chemo-/regioselectivity and high to excellent stereoselectivity. Computational mechanistic studies elucidate the origin of the stereochemical outcome and the chemoselectivity, in which the thermostability of these cycloaddition products is the major factor.

Introduction

The catalytic asymmetric 1,3-dipolar cycloaddition (1,3-DC) reactions of azomethine ylides are one of the most powerful and versatile strategies for the construction of enantioenriched nitrogen-containing heterocyclic compounds,^{1,2} which serve as the privileged skeletons widely distributed in a range of bioactive natural products and pharmaceutical molecules.³ As a consequence, great efforts have been devoted to developing various novel catalytic systems for further extension of the applicable range of this methodology.⁴ Among the currently reported examples, alkenes bearing at least one electron-withdrawing group to activate alkenes (dipolarophiles) have been commonly and generally used as dipolarophiles. In sharp contrast, alkenes without any electron-withdrawing substituents rarely play a role of dipolarophiles in the catalytic asymmetric 1,3-dipolar cycloaddition reaction with azomethine ylides,⁵ which may be ascribed to the absence of LUMO activation of alkenes (Scheme 1a). It was not until 2009 that this challenge was first attempted by the Martin

group.⁶ They reported a seminal asymmetric version of transition metal-catalyzed 1,3-dipolar cycloaddition reactions between fullerene C₆₀ and azomethine ylides, successfully constructing an array of enantioenriched pyrrolidinofullerenes in high yields with excellent enantio-selectivities under mild reaction conditions (Scheme 1b). The strain of the curved double bond in C₆₀ serving as the 2π -component provides the crucial driving force for the event of 1,3-dipolar cycloaddition.⁷ Later, Waldmann⁸ and our group⁹ independently developed fulvene-involved catalytic asymmetric higher-order [3 + 6] cycloaddition reactions of azomethine ylides, in which electron-rich fulvenes acted as 6π -components and the intrinsic nonbenzenoid aromatic character¹⁰ of fulvenes offers the major driving force. Despite these advances, such catalytic synthetic transformations with electron-rich olefines are still of great challenge and have remained in an infant stage. Therefore, further investigation of other types of olefines without any electron-withdrawing groups as dipolarophiles in azomethine ylide-involved catalytic asymmetric 1,3-dipolar cycloadditions was in high demand and desirable.

Benzofulvenes, a kind of synthon having semi-aromatic characteristics, have been mainly employed in the synthesis of polymeric compounds and transition-metal-complexes.¹¹ In comparison, the utilization of these synthons to construct small molecules was rarely reported, particularly in a catalytic asymmetric manner,¹² which may be ascribed to the low activity of the diene in the benzofulvene. In 2016, Jørgensen introduced an electron-withdrawing group at the 3-position of the benzofulvene to enhance the reactivity of the exocyclic double bond, which served as a 2π -component to react with 2,4-dienals or dimethyl bromomalonate in the presence of chiral catalysts.^{12a,b} With the aid of electron-withdrawing groups, a series of spiroindenes bearing

^aEngineering Research Center of Organosilicon Compounds & Materials, Ministry of Education, College of Chemistry and Molecular Sciences, Wuhan University, Wuhan, 430072, China. E-mail: cjwang@whu.edu.cn

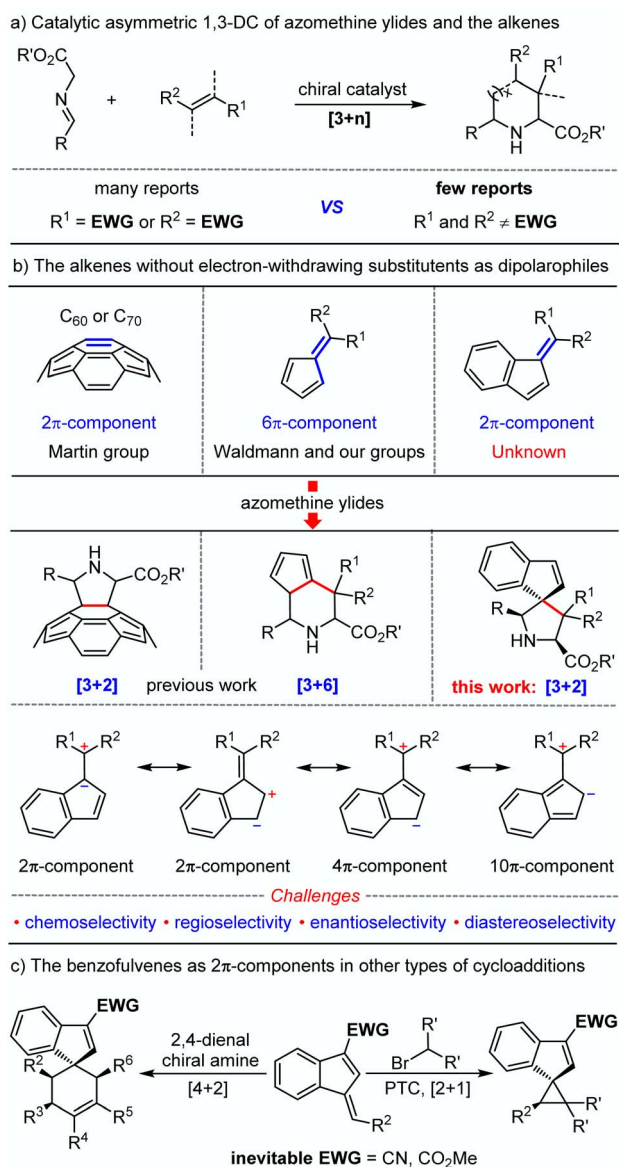
^bState Key Laboratory of Organometallic Chemistry, Shanghai Institute of Organic Chemistry, Shanghai, 230021, China

^cDepartment of Chemistry and Guangdong Provincial Key Laboratory of Catalysis, Southern University of Science and Technology, Shenzhen, 518055, China. E-mail: oscarchung@sustech.edu.cn

† Electronic supplementary information (ESI) available. CCDC 2234947 and 2256257. For ESI and crystallographic data in CIF or other electronic format see DOI: <https://doi.org/10.1039/d3sc00435j>

‡ These three authors contributed equally.





Scheme 1 (a and b) Catalytic asymmetric 1,3-DC of azomethine ylides and alkenes. (c) Other cycloaddition reactions with benzofulvene derivatives incorporating electron-withdrawing substituents.

an all-carbon quaternary stereocenter were smoothly formed in excellent yield and diastereoselectivity (Scheme 1c). In continuation of our research interest in azomethine ylide-involved catalytic asymmetric 1,3-dipolar cycloaddition reactions,^{2*ij*,13} we envisioned that benzofulvenes without any electron-withdrawing substituents may serve as 2 π type dipolarophiles to participate in azomethine ylide-involved catalytic asymmetric 1,3-dipolar cycloadditions to enable the modular assembly of enantioenriched spiro-pyrrolidine derivatives. Nevertheless, several challenges may exist in the design: (1) whether reactivity driven by the intrinsic nonbenzenoid aromatic characteristic is enough for the novel dipolarophiles (benzofulvenes) because electron-withdrawing groups were inevitable in the previous [2 + 1] and [4 + 2] cycloadditions promoted by organocatalysts; (2) the control of chemo- and regioselectivity due

to the existence of diverse electronic resonance structures in benzofulvene; (3) the construction of two contiguous all carbon quaternary centers including a challenging spiro chirality in a catalytic asymmetric manner.

Herein, we reported an unprecedented catalytic asymmetric 1,3-dipolar cycloaddition reaction of azomethine ylides and benzofulvenes, in which benzofulvenes without any electron-withdrawing substituents were capable to act as efficient 2 π dipolarophiles for the high-efficiency synthesis of a series of multi-substituted enantioenriched pyrrolidine derivatives bearing a spiroindene molecular architecture which is prevalent in diverse active pharmaceutical ingredients and natural products.¹⁴

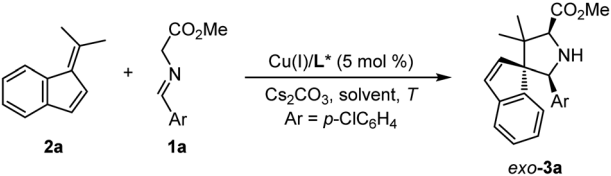
Results and discussion

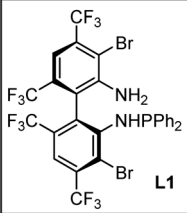
Reaction development and optimization

Initially, we choose readily available benzofulvene **2a** and aldimine ester **1a** as the model substrate and Cs₂CO₃ as the base to examine the feasibility of this design. As shown in Table 1, the optimal chiral ligand TF-BiphamPhos^{9,15} in the fulvene-involved catalytic asymmetric 1,3-dipolar [3 + 6] cycloaddition was first examined in dichloromethane at room temperature. Unfortunately, no desired spiroheterocyclic product was observed (Table 1, entry 1). We turned our attention to the investigation of other types of chiral ligands. Chiral bisphosphine ligands (**L2**, **L3**, **L4**) did make the corresponding reaction happen, but with unsatisfactory yield and stereoselectivity (Table 1, entries 2–4). Subsequently, a series of chiral N–P ligands Phosferrox **L5**–**L9** were further evaluated (Table 1, entries 5–9). These experimental results suggested that the chiral ligand **L6** derived from *L*-valine represents a better performance, delivering the desired cycloadduct **3a** in 98% yield with 16 : 1 *dr* and 87% *ee* (Table 1, entry 6). To further improve the stereoselectivity, we explored other experimental conditions. Switching Cu(I) with Ag(I) was proved to be ineffective and can be detrimental to diastereoselectivity (Table 1, entry 10). Reducing the reaction temperature to 10 °C led to an obvious increase in the enantioselectivity at the expense of diastereoselectivity (Table 1, entry 11). The reaction became very sluggish when the temperature was reduced further (Table 1, entry 12). Solvent-screening (Table 1, entries 13–19) revealed that Et₂O was the best choice, affording a satisfactory outcome (81% yield, 18 : 1 *dr*, 96% *ee*; Table 1, entry 15), which was determined as the optimal reaction condition in this study.

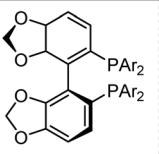
Substrate scope

With the optimal reaction conditions in hand, we commenced examining the generality of this catalytic asymmetric 1,3-dipolar cycloaddition by treating benzofulvene **2a** with different aldimine esters, **1a**–**1n**. As shown in Table 2, a variety of aldimine esters bearing electron-withdrawing, electron-neutral and electron-donating substituents at the *ortho*-, *meta*- or *para*-position of the aromatic ring could react successfully with **2a**, affording the corresponding cycloadducts **3a**–**3i** in good yields (67–98%) with excellent stereoselectivity (10 : 1–20 : 1 *dr*, 91–98% *ee*; entries 1–9). With further extension from the phenyl ring to a fused aromatic

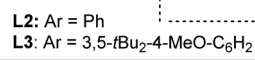
Table 1 Optimization of reaction conditions^a




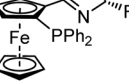
L1



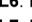
L2: Ar = Ph



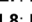
L3: Ar = 3,5-tBu₂-4-MeO-C₆H₂



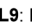
L4: (S)-BINAP



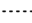
L5: R = Et



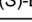
L6: R = *i*Pr



L7: R = *t*Bu



L8: R = Bn



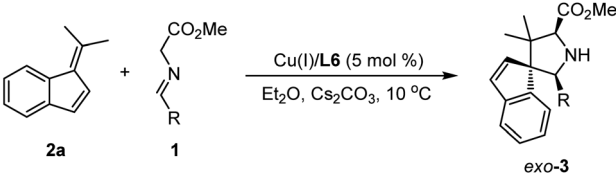
L9: R = Ph

Entry	L*	T (°C)	Solvent	Yield ^b (%)	dr ^c	ee ^d (%)
1	L1	25	DCM	5	ND	ND
2	L2	25	DCM	88	9 : 1	40
3	L3	25	DCM	40	5 : 1	85
4	L4	25	DCM	93	7 : 1	20
5	L5	25	DCM	29	11 : 1	89
6	L6	25	DCM	98	16 : 1	87
7	L7	25	DCM	56	7 : 1	85
8	L8	25	DCM	93	15 : 1	89
9	L9	25	DCM	98	12 : 1	87
10 ^e	L6	25	DCM	80	2 : 1	87
11	L6	10	DCM	76	14 : 1	96
12	L6	0	DCM	5	—	—
13	L6	10	DCE	77	20 : 1	87
14	L6	10	THF	93	14 : 1	90
15	L6	10	Et ₂ O	81	18 : 1	96
16	L6	10	Toluene	98	12 : 1	96
17	L6	10	CF ₃ CH ₂ OH	Trace	—	—
18	L6	10	CH ₃ CN	Trace	—	—
19	L6	10	MeOH	Trace	—	—

^a Unless otherwise noted, all reactions were carried out with 0.4 mmol **1a**, 0.2 mmol **2a**, 0.01 mmol [Cu(I)]/L and 0.2 mmol of Cs₂CO₃ in 2 mL of solvent 10–16 h, Cu(I) = Cu(CH₃CN)₄BF₄. ^b Isolated yield. ^c The dr value was determined by the crude ¹H NMR. ^d ee value was determined by HPLC analysis. ^e AgOAc was used. ND = Not determined.

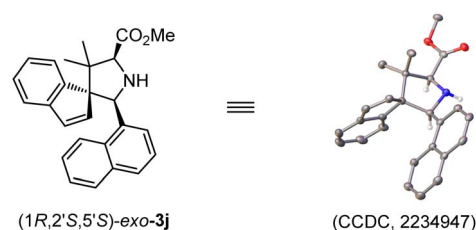
ring (bulky 1-naphthyl **1j** and 2-naphthyl **1k**), an excellent level of enantioselectivity (96 and 95% ee) could still be achieved with moderate to good yield (56 and 98% yield) and diastereoselectivity (7 : 1 and 10 : 1 dr; entries 10 and 11). In addition, subjecting heteroaromatic aldehyde-derived imine ester **1l** and **1m** to this catalytic system, the desired cycloadducts **3l** and **3m** were isolated in acceptable yields with high to excellent enantioselectivity (entries 12 and 13). It is worth noting that the challenging and less reactive aldimine ester **1n** derived from cyclohexylaldehyde was proven to be a suitable precursor of azomethine ylide, furnishing the cycloadduct **3n** in 72% yield with 20 : 1 dr and 97% ee (entry 14). The absolute configuration of **3j** was unambiguously determined as (1*R*,2'*S*,5'*S*) by the X-ray diffraction analysis (Fig. 1).¹⁶

Having established the scope of aldimine esters, we then set out to evaluate the scope of benzofulvenes **2** with aldimine ester **1a**. As

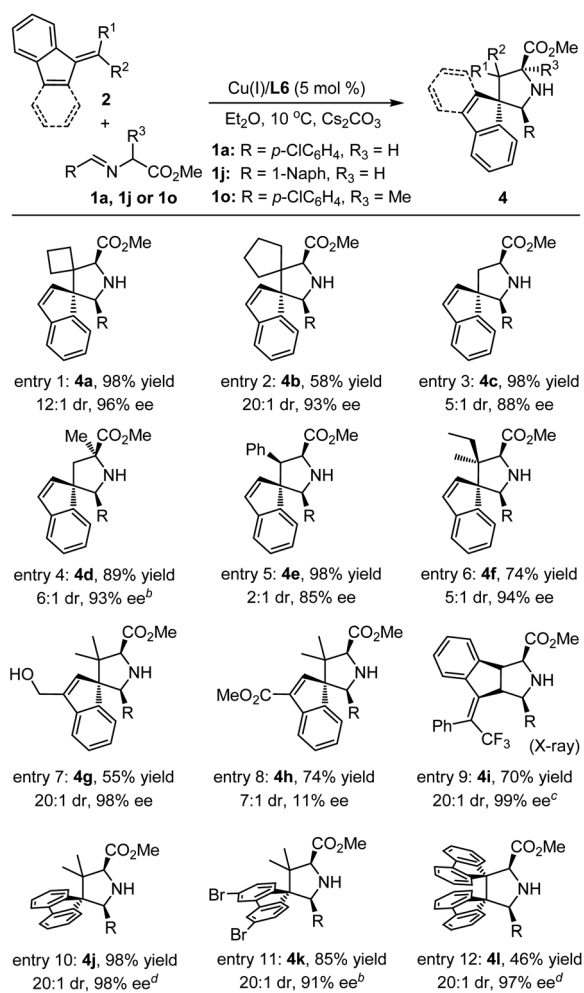
Table 2 Substrate scope of imine esters^a


Entry	R	3	Yield ^b (%)	dr ^c	ee ^d (%)
1	<i>p</i> -ClC ₆ H ₄	3a	81	18 : 1	96
2	<i>m</i> -ClC ₆ H ₄	3b	67	12 : 1	95
3	<i>p</i> -BrC ₆ H ₄	3c	98	20 : 1	97
4	<i>p</i> -CF ₃ C ₆ H ₄	3d	96	15 : 1	98
5	Ph	3e	71	10 : 1	94
6	<i>p</i> -MeC ₆ H ₄	3f	88	15 : 1	92
7 ^e	<i>o</i> -MeC ₆ H ₄	3g	76	20 : 1	97
8 ^f	<i>m</i> -MeC ₆ H ₄	3h	72	15 : 1	91
9 ^f	<i>p</i> -MeOC ₆ H ₄	3i	79	18 : 1	96
10	1-Naphthyl	3j	56	7 : 1	96
11 ^f	2-Naphthyl	3k	98	10 : 1	95
12	2-Thienyl	3l	98	15 : 1	96
13	2-Furyl	3m	58	9 : 1	86
14	Cyclohexyl	3n	72	20 : 1	97

^a Unless otherwise noted, all reactions were carried out with 0.4 mmol **1**, 0.2 mmol **2a**, 0.01 mmol Cu(I)/L6 and 0.2 mmol of Cs₂CO₃ in 2 mL of Et₂O for 24 h, Cu(I) = Cu(CH₃CN)₄BF₄. ^b Isolated yield. ^c The dr value was determined by the crude ¹H NMR. ^d ee value was determined by HPLC analysis. ^e *t*BuOK was used instead of Cs₂CO₃. ^f The reaction was run at 20 °C.

Fig. 1 X-Ray Structure of (1*R*,2'*S*,5'*S*)-**3j**.

outlined in Table 3, employing symmetrical cyclobutanone and cyclopentanone-derived benzofulvenes **2b** and **2c** as dipolarophiles, the corresponding cycloadducts **4a** and **4b** containing two contiguously spirocyclic skeletons could be formed smoothly in good to excellent yield with good stereoselectivity (entries 1–2). Notably, when the highly active benzofulvene **2d** bearing a terminal alkene moiety was selected as the dipolarophile, the corresponding cycloaddition could occur in a satisfactory result, even when the more challenging α -Me-substituted aldimine ester **1o** was employed in this system (entries 3 and 4). Switching the symmetrical ketone/aldehyde with unsymmetrical 2-butanone or benzaldehyde, a similar reactivity and enantiocontrol were also achieved with acceptable diastereoselectivity (entries 5 and 6). To further explore the compatibility of this reaction, a series of

Table 3 Substrate scope of benzofulvenes^a

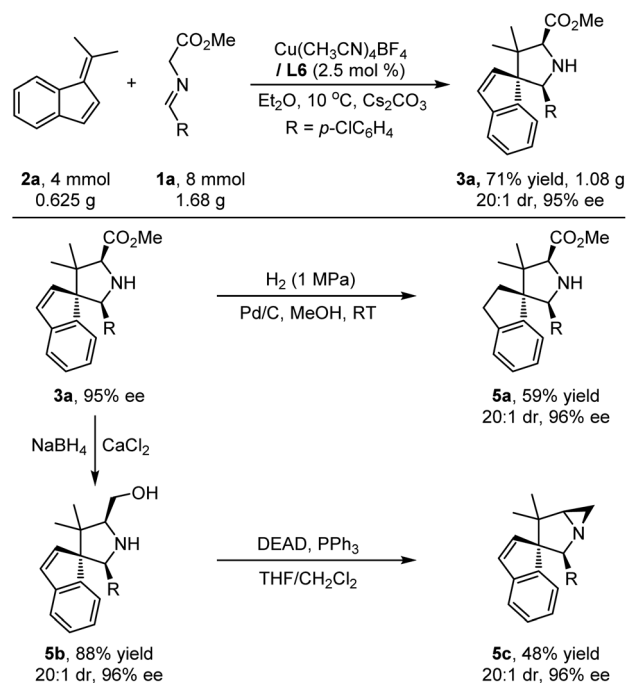
^a All reactions were carried out with 0.4 mmol **1** and 0.2 mmol **2**, 0.01 mmol Cu/L6 and 0.2 mmol Cs_2CO_3 in 2 mL of Et_2O for 16 h, $\text{Cu(I)} = \text{Cu}(\text{CH}_3\text{CN})_4\text{BF}_4$. Isolated yield. The dr value was determined by the crude ^1H NMR, and the ee value was determined by HPLC analysis. ^b The reaction was run at $0\text{ }^\circ\text{C}$. ^c $\text{R} = 1 - \text{Naph}$. ^d The reaction was run at $20\text{ }^\circ\text{C}$.

substituent groups possessing different electronic properties on the benzofulvene were further investigated. The corresponding experimental results indicated that the electron-donating hydroxymethyl group positioned at the endocyclic $\text{C}=\text{C}$ bond had little impact on the reactivity and selectivity (entry 7). The electron-withdrawing CO_2Me group located at the endocyclic $\text{C}=\text{C}$ bond indeed enhanced the polarization of the exocyclic $\text{C}=\text{C}$ bond, affording the corresponding spiro heterocyclic adduct **4h** in good yield albeit with unsatisfactory stereoselectivity (7 : 1 dr and 11% ee) and yield (74%) (entry 8). Switching the electron-withdrawing group from the endocyclic double bond to the exocyclic double bond would directly result in the change of regioselectivity. The endocyclic double bond reacted with azomethine ylides, giving rise to the corresponding fused cycloadduct **4i** in moderate yield (70%) with excellent stereoselectivity (20 : 1 dr, 99% ee), which revealed

that the inductive effect of the CF_3 group was stronger than the driving force from the reduced intrinsic nonbenzenoid aromatic character of the benzofulvene **2i** (entry 9). The absolute configuration of **4i** was unambiguously determined as (1*R*,3*S*,3*aR*,8*aS*,*E*) by the X-ray diffraction analysis.¹⁶ In addition to indene-derived benzofulvenes, more bulky 9-fluorenone-derived olefins proved to be viable substrates for this catalytic asymmetric cycloaddition reaction, producing the desired cycloadducts **4j** and **4k** in high yield (98%, 85%) with excellent diastereoselectivity (20 : 1 dr) and enantiomeric excess (98%, 91%, entries 10 and 11). Encouraged by these results, a more challenging dipolarophile **2l** bearing double bulkier fluorene moieties was investigated to further determine the compatibility of this catalytic system. Gratifyingly, the corresponding cycloaddition reactions still underwent smoothly to deliver the desired adducts **4l** in 46% yield with exclusive diastereoselectivity and excellent enantioselectivity (entry 12).

Scale-up experiments and synthetic application

To demonstrate the practicability and synthetic utility of the current methodology, we performed a gram-scale reaction of **1a** and **2a** under slightly modified reaction conditions with reduced catalyst loading (2.5 mol%). As shown in Scheme 2, a comparable yield (71%) and stereoselectivity (20 : 1 dr, 95% ee) were observed. Under 1 MPa of H_2 , Pd/C-catalyzed reduction of the endocyclic double bond of the product **3a** could be realized, providing the target compound **5a** in 59% yield with maintained stereoselectivity (20 : 1 dr, 96% ee). Treating cycloadduct **3a** with NaBH_4 and CaCl_2 could selectively reduce the ester group of **3a** efficiently, and the corresponding amino alcohol **5b** was isolated in high yield with excellent stereoselectivity, which could



Scheme 2 Scale-up experiments and synthetic elaborations.

be further stereospecifically transformed into more complex product **5c** bearing a biologically important 1-azabicyclo[3.1.0]hexane heterocyclic moiety.¹⁷

Computational study of the reaction mechanism for the formation of **3a**

To understand the origin of the stereo-, chemo-, and regioselective 1,3-dipolar cycloaddition reaction of benzofulvenes catalyzed by Cu(I)-L6, systematic DFT calculations (the PCM M06-L//M06-L method mainly) were carried out.^{18–20} As shown in Fig. 2A, there are two possible coordination models (**L6-U** and **L6-D**) for a four-coordinate intermediate containing Cu(I)-L6 and the deprotonated **1a** (dipole). **L6-D** was computed to be more stable than **L6-U** by 4.1 kcal mol⁻¹ in the solution by the PCM M06-L//M06-L method, due to more steric congestion between the ferrocene group in **L6** and a larger aryl substituent in the dipole (more C–H repulsion in **L6-U**, see Fig. 2A and S3†). In addition, the steric map²¹ (Fig. 2B) shows that the *i*-Pr group in **L6** occupies the upper coordination sphere and should exclude the cycloaddition of benzofulvene substrates on the top side. Therefore, our results show that the dipolarophile substrate preferentially attacks the dipole from the bottom side (Fig. 2C).

Fig. 2 and 3 further depict two energetically favorable [3 + 2] cycloaddition pathways for the substrate **2a**. Our DFT calculations

show that the formation of these favorable major and minor cycloaddition products (**A1** and **A2**) is a two-step process. Addition of **2a** to the four-coordinate intermediate **L6-D** (or **L6-U**) forms a less stable intermediate ^D**IN1-A1** (or ^U**IN1-A2**; $\Delta G_{\text{soln}} = 5.2\text{--}5.8$ kcal mol⁻¹). Then, the first C₁–C₃ bond addition from an electron-rich C₁ of the dipole ($q(\text{C}_1)$: -0.23 , Fig. 2A) to the C₃ site of the dipolarophile occurs *via* ^D**TS1-A1** or ^U**TS1-A2** with a barrier of 16.5 or 19.9 kcal mol⁻¹ to afford a less stable zwitterionic intermediate ^D**IN2-A1** or ^U**IN2-A2** ($\Delta G_{\text{soln}} = 14.1$ or 18.9 kcal mol⁻¹), respectively. Such regioselective addition to the C₃ position is kinetically and thermodynamically much more favorable than the addition to another C₄ position of the dipolarophile by at least 1.6 kcal mol⁻¹ (Fig. 3 and S1†), due to stabilization of the formal resultant carb-anion by π -conjugation interaction with the aromatic ring (*c.f.* ^D**IN2-A1**).

Afterward, ^D**IN2-A1** and ^U**IN2-A2** undergo the second C₂–C₄ bond addition to form the major cycloadduct intermediate ^D**IN3-A1** and the minor cycloadduct ^U**IN3-A2** *via* ^D**TS2-A1** and ^U**TS2-A2**, respectively. This final cyclization step in both [3 + 2] pathways is suggested to be the rate-determining step with a barrier of 22.0–24.3 kcal mol⁻¹. ^D**TS2-A1** leading to the major product ^D**IN3-A1** has a lower barrier than ^U**TS2-A2** forming ^U**IN3-A2** ($\Delta\Delta G_{\text{soln}}^{\ddagger} = \sim 2.3$ kcal mol⁻¹ and $\Delta\Delta E_{\text{soln}}^{\ddagger} = \sim 0.8$ kcal mol; Fig. 2 and 3), which qualitatively explains the observed stereo- and regiochemistry. The entropy effect (~ 1.1 kcal mol⁻¹) and a smaller distortion energy²² ($\Delta\Delta E_{\text{dist, soln}} = \sim 1.5$ kcal mol;

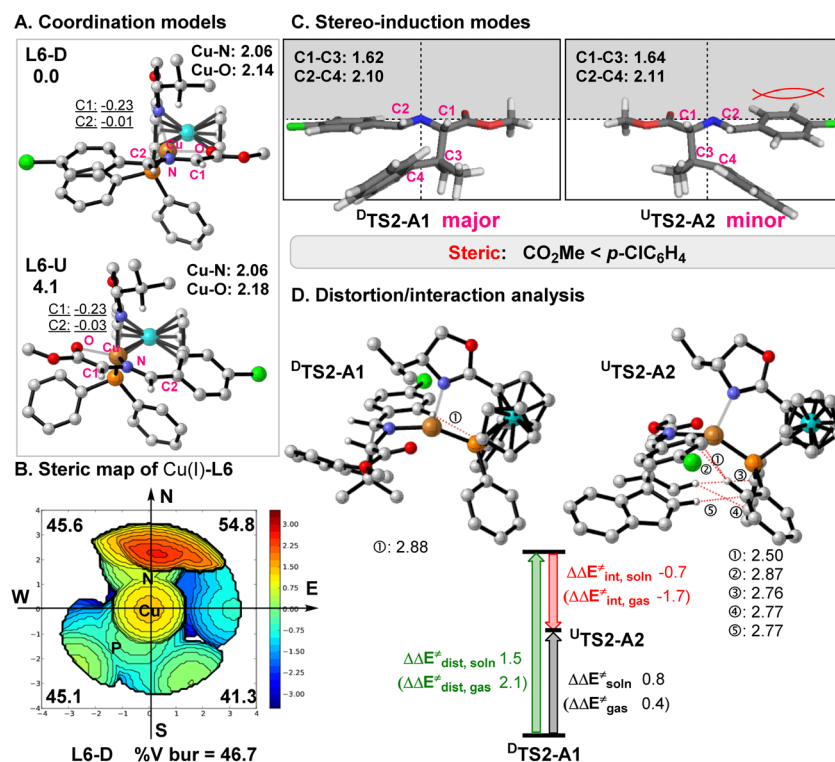


Fig. 2 (A) Two optimized coordination modes (**L6-D** and **L6-U**) of the active four-coordinate Cu(I) intermediate in the gas phase by the M06-L method with the key bond distances. The relative free energies and NPA charge for the key atoms in diethylether solution by the PCM M06-L//M06-L method are given. (B) Steric map of the Cu(I)-L6 part from the optimized **L6-D** with the computed buried volumes. (C) Stereo-induction modes for the enantioselectivity. (D) Distortion/interaction analysis for the Cu-catalyzed [3 + 2] cycloaddition of **2a** with the key repulsions between substrates and **L6** (in angstrom).

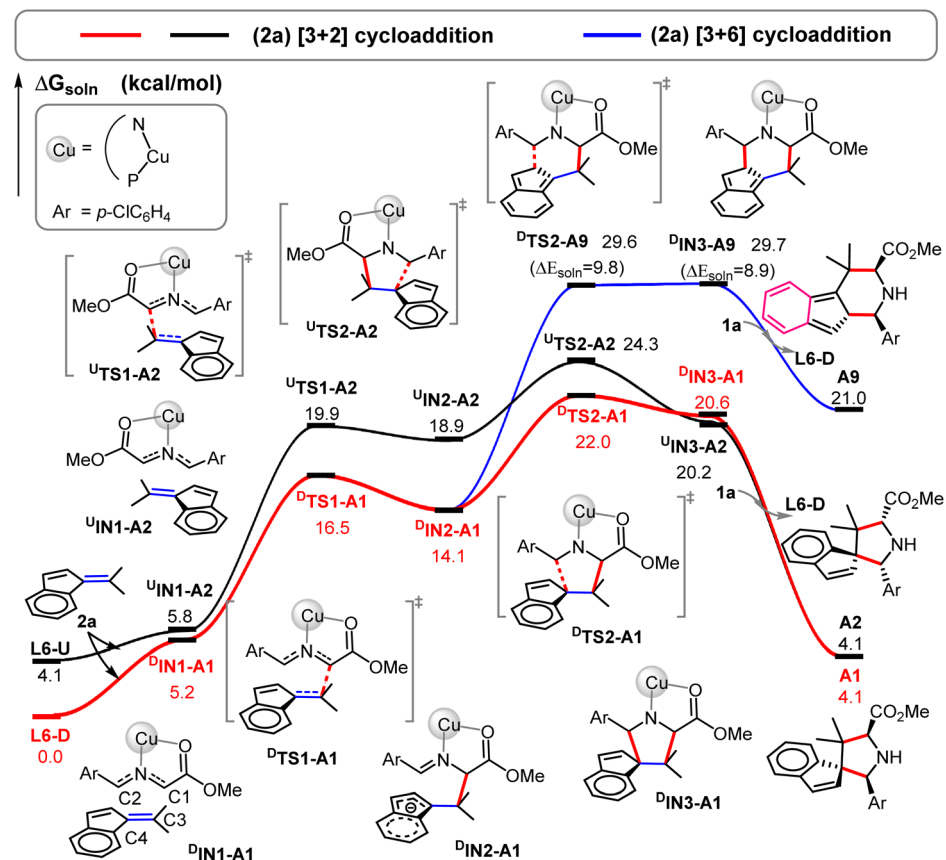


Fig. 3 Free energy profiles for the Cu-catalyzed [3 + 2] (in red and black solid lines) and [3 + 6] (in the blue solid line) cycloadditions of **2a** in the solution by the PCM M06-L//M06-L method.

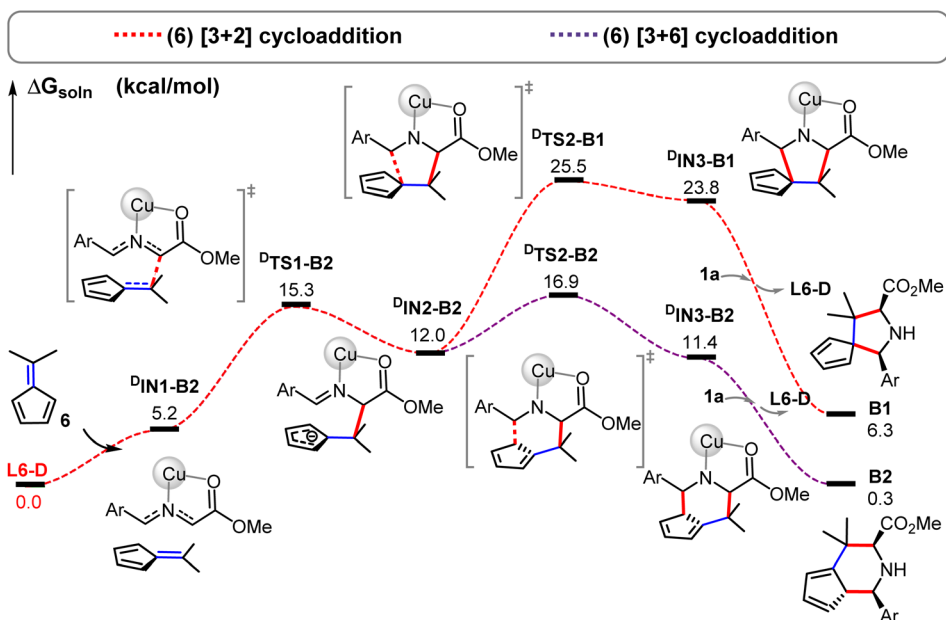


Fig. 4 Free energy profiles for the Cu-catalyzed [3 + 2] (in the red dashed line) and [3 + 6] (in the purple dashed line) cycloaddition reactions of substrate **6** in the solution by the PCM M06-L//M06-L method.

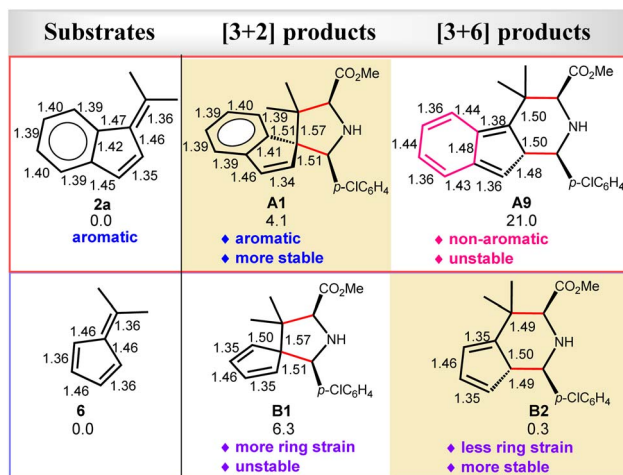


Fig. 5 The key bond distances (in angstrom) of the optimized substrates (**2a** and **6**) and their corresponding cycloaddition products by the M06-L method (those optimized by the M06-2X method given in Fig. S4†). The relative free energies (kcal mol^{-1}) of these cycloaddition products in the solution by the PCM M06-L//M06-L method are also given.

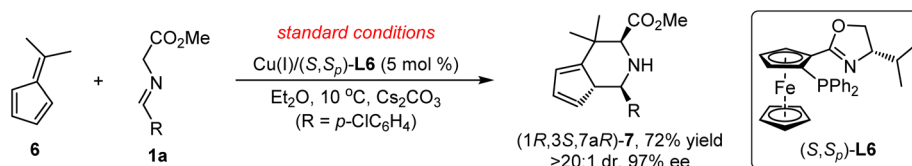
Fig. 2d) play the key roles in controlling the enantioselectivity, whereas the solvation also slightly favors the major-type cyclization TS ($\sim 0.4 \text{ kcal mol}^{-1}$). In addition, more congestion between the substrates and ligand were found in ${}^{\text{U}}\text{TS2-A2}$ than ${}^{\text{D}}\text{TS2-A1}$ (Fig. 2d). Finally, ligand exchange of ${}^{\text{D}}\text{IN3-A1}$ (or ${}^{\text{U}}\text{IN3-A2}$) with another **1a** substrate can regenerate the active species (**L6-D**) as well as release the cycloaddition product **A1** (or **A2**) and energy.

In comparison, our calculations reveal that ${}^{\text{D}}\text{IN2-A1}$ requires a much larger barrier ($29.6 \text{ kcal mol}^{-1}$) for the [3 + 6] cycloaddition (branching) pathway *via* ${}^{\text{D}}\text{TS2-A9}$ by $7.6 \text{ kcal mol}^{-1}$, compared to the most-favorable major pathway *via* ${}^{\text{D}}\text{TS2-A1}$. Remarkably, the [3 + 6] cycloadduct intermediate ${}^{\text{D}}\text{IN3-A9}$ is found to be highly unstable ($\Delta G_{\text{soln}} = 29.7 \text{ kcal mol}^{-1}$). It should be noted that the [3 + 6] cycloaddition induces π -bond shifting and, thus, transforms the aromatic ring of **2a** into the non-aromatic ring in the highly unstable [3 + 6] cycloaddition product **A9** ($\Delta G_{\text{soln}} = 21.0 \text{ kcal mol}^{-1}$). As **A9** is thermodynamically much unstable than the [3 + 2] cycloaddition products **A1** and **A2** ($\Delta G_{\text{soln}} = 4.1 \text{ kcal mol}^{-1}$), thermostability of these cycloaddition products is the major factor in the chemoselective [3 + 2] cycloaddition and excludes the formation of the unstable [3 + 6] cycloadducts with benzofulvenes (Fig. 3–5).

Interestingly, our DFT calculations predict that the same cycloaddition reaction with the simplest fulvene substrate **6** favors the [3 + 6] cycloaddition in this catalytic system (Scheme 3), instead of the [3 + 2] cycloaddition (Fig. 4 and 5). Its reaction barrier for the [3 + 2] cycloaddition ($25.5 \text{ kcal mol}^{-1}$ *via* ${}^{\text{D}}\text{TS2-B1}$) is much higher than that for the [3 + 6] cycloaddition ($16.9 \text{ kcal mol}^{-1}$ *via* ${}^{\text{D}}\text{TS2-B2}$) by $8.6 \text{ kcal mol}^{-1}$. Notably, the [3 + 2] cycloadduct intermediate ${}^{\text{D}}\text{IN3-B1}$ becomes thermodynamically less stable than the [3 + 6] cycloadduct intermediate ${}^{\text{D}}\text{IN3-B2}$ by $12.4 \text{ kcal mol}^{-1}$. Likewise, the [3 + 2] product **B1** (5/5-spiro-ring; $\Delta G_{\text{soln}} = 6.3 \text{ kcal mol}^{-1}$) is also less stable than the [3 + 6] product **B2** (5/6-fused-ring; $\Delta G_{\text{soln}} = 0.3 \text{ kcal mol}^{-1}$) by $6.0 \text{ kcal mol}^{-1}$. Apparently, less ring strain and more substituted alkene part should gain more thermostability in the 5/6-fused ring ([3 + 6] cycloadduct) than the 5/5-spiro ring ([3 + 2] cycloadduct). Therefore, the higher thermostability in the simple 5/6-fused ring should be the key factor in dictating chemoselective [3 + 6] cycloaddition with fulvenes. In comparison, the [3 + 6] product (6/5/6-fused-ring) for benzofulvene **2a** loses the aromatic stability and has more steric congestion between one methyl and phenyl groups (due to the roughly-planar geometry, Fig. S3†), which renders highly unstable [3 + 6] cycloadduct as well as raises its reaction barrier ($29.6 \text{ kcal mol}^{-1}$). In contrast, thermochemistry of the [3 + 2] product for **2a** is slightly more favorable than that for **6**, which promotes the [3 + 2] cycloaddition with **2a**. These combined experimental and computational results demonstrate interesting substrate-dependent/switching chemoselective 1,3-dipolar cycloadditions.

Conclusions

In conclusion, combining the intrinsic nonbenzenoid aromatic characteristic of benzofulvenes, we have successfully developed catalytic asymmetric [3 + 2] cycloaddition between azomethine ylides and electron-rich benzofulvenes without any electron-withdrawing substituents for the first time. Such efficient reaction gives access to a variety of multi-substituted chiral spiro pyrrolidine derivatives containing two contiguous all carbon quaternary centers in high yields with exclusive chemo-/regioselectivity and high to excellent stereoselectivity. Extensive density functional theory (DFT) calculations not only elucidated the reaction mechanism of the formation of the cycloadducts, but also demonstrated that the excellent chemo-/regioselectivity is dependent on the thermostability of the corresponding cycloaddition products.



Scheme 3 Experimental proof of $\text{Cu(I)/(S,S}_p\text{)-L6}$ -catalyzed [3 + 6] cycloaddition of aldimine ester **1a** with fulvene **6** as the dipolarophile.

Data availability

The datasets supporting this article have been uploaded as part of the ESI.†

Author contributions

C.-J. W. conceived and designed the research. C.-J. W. and X. C. directed the project. X. C. and X.-T. L. performed the research. F. L., Y. Y., L. W. C. performed the DFT calculations. X. C., L. W. C. and C.-J. W. co-wrote the paper. All authors analysed the data, discussed the results, commented on the manuscript, collected data and prepared the ESI.†

Conflicts of interest

There are no conflicts to declare.

Acknowledgements

This work was supported by the NSFC (22071186, 22101216, 22073067, 21933003, 22193020, and 22193023), the Hubei Province Natural Science Foundation (2020CFA036), China Postdoctoral Science Foundation (2021M702514), the Fundamental Research Funds for the Central Universities (2042022kf1180), the Shenzhen Nobel Prize Scientists Laboratory Project (C17783101) and Guangdong Provincial Key Laboratory of Catalytic Chemistry (2020B121201002). The authors thank Dr Ran Zhang from the Core Facility of Wuhan University for his generous support in the X-ray structure analysis and the Center for Computational Science and Engineering at the Southern University of Science and Technology and CHEM HPC at SUSTech for partly supporting this work.

Notes and references

- (a) R. Huisgen, *Angew. Chem., Int. Ed.*, 1963, **2**, 565–598; (b) S. L. Schreiber, *Science*, 2000, **287**, 1964–1969; (c) A. Padwa and W. H. Pearson, *Synthetic Applications of 1,3-Dipolar Cycloaddition Chemistry Toward Heterocycles and Natural Products*, ed. H. Feuer, Wiley-VCH, 2002.
- For selected reviews on catalytic asymmetric 1,3-dipolar cycloadditions, see: (a) I. Coldham and R. Hufton, *Chem. Rev.*, 2005, **105**, 2765–2810; (b) C. Najera and J. M. Sansano, *Angew. Chem., Int. Ed.*, 2005, **44**, 6272–6276; (c) G. Pandey, P. Banerjee and S. R. Gadre, *Chem. Rev.*, 2006, **106**, 4484–4517; (d) H. Pellissier, *Tetrahedron*, 2007, **63**, 3235–3285; (e) M. Álvarez-Corral, M. Muñoz-Dorado and I. Rodríguez-García, *Chem. Rev.*, 2008, **108**, 3174–3198; (f) L. M. Stanley and M. P. Sibi, *Chem. Rev.*, 2008, **108**, 2887–2902; (g) J. Adrio and J. C. Carretero, *Chem. Commun.*, 2011, **47**, 6784–6794; (h) J. Adrio and J. C. Carretero, *Chem. Commun.*, 2014, **50**, 12434–12446; (i) T. Hashimoto and K. Maruoka, *Chem. Rev.*, 2015, **115**, 5366–5412; (j) X. Fang and C.-J. Wang, *Org. Biomol. Chem.*, 2018, **16**, 2591–2601; (k) L. Wei, X. Chang and C.-J. Wang, *Acc. Chem. Res.*, 2020, **53**, 1084–1100.
- (a) K. Ding, Y. Lu, Z. Nikolovska-Coleska, S. Qiu, Y. Ding, W. Gao, J. Stuckey, K. Krajewski, P. P. Roller, Y. Tomita, D. A. Parrish, J. R. Deschamps and S. Wang, *J. Am. Chem. Soc.*, 2005, **127**, 10130–10131; (b) J. P. Michael, *Nat. Prod. Rep.*, 2008, **25**, 139–165; (c) S. D. Roughley and A. M. Jordan, *J. Med. Chem.*, 2011, **54**, 3451–3479; (d) M. Setoguchi, S. Iimura, Y. Sugimoto, Y. Yoneda, J. Chiba, T. Watanabe, F. Muro, Y. Iigo, G. Takayama, M. Yokoyama, T. Taira, M. Aonuma, T. Takashi, A. Nakayama and N. Machinaga, *Bioorg. Med. Chem.*, 2013, **21**, 42–61; (e) Y. Zhao, L. Liu, W. Sun, J. Lu, D. McEachern, X. Li, S. Yu, D. Bernard, P. Ochsenein, V. Ferey, J.-C. Carry, J. R. Deschamps, D. Sun and S. Wang, *J. Am. Chem. Soc.*, 2013, **135**, 7223–7234; (f) M. Kuhnert, A. Blum, H. Steuber and W. E. Diederich, *J. Med. Chem.*, 2015, **58**, 4845–4850; (g) Y. Zhao, A. Aguilar, D. Bernard and S. Wang, *J. Med. Chem.*, 2015, **58**, 1038–1052; (h) L. Shu, C. Gu, D. Fishlock and Z. Li, *Org. Process Res. Dev.*, 2016, **20**, 2050–2056; (i) J. Hartung, S. N. Greszler, R. C. Klix and J. M. Kallemeyn, *Org. Process Res. Dev.*, 2019, **23**, 2532–2537; (j) T. Ince, R. Serttas, B. Demir, H. Atabey, N. Seferoglu, S. Erdogan, E. Sahin, S. Erat and Y. Nural, *J. Mol. Struct.*, 2020, **1217**, 128400; (k) K. V. Kudryavtsev, M. N. Sokolov, E. E. Varpetyan, A. A. Kirsanova, N. I. Fedotcheva, N. L. Shimanovskii and T. A. Fedotcheva, *ChemistrySelect*, 2020, **5**, 11467–11470; (l) X.-J. Zou, W.-L. Yang, J.-Y. Zhu and W.-P. Deng, *Chin. J. Chem.*, 2020, **38**, 435–438.
- For the most recent examples of transition-metal-catalyzed asymmetric 1,3-dipolar cycloadditions, see: (a) I. N. Chaithanya Kiran, K. Fujita, S. Tanaka and M. Kitamura, *ChemCatChem*, 2020, **12**, 5613–5617; (b) X. Cheng, D. Yan, X.-Q. Dong and C.-J. Wang, *Asian J. Org. Chem.*, 2020, **9**, 1567–1570; (c) H. Cui, K. Li, Y. Wang, M. Song, C. Wang, D. Wei, E.-Q. Li, Z. Duan and F. Mathey, *Org. Biomol. Chem.*, 2020, **18**, 3740–3746; (d) S. Furuya, K. Kanemoto and S.-i. Fukuzawa, *J. Org. Chem.*, 2020, **85**, 8142–8148; (e) E. Garcia-Mingueens, V. Selva, O. Larranaga, C. Najera, J. M. Sansano and A. de Cozar, *ChemCatChem*, 2020, **12**, 2014–2021; (f) J.-P. Tan, X. Li, Y. Chen, X. Rong, L. Zhu, C. Jiang, K. Xiao and T. Wang, *Sci. China: Chem.*, 2020, **63**, 1091–1099; (g) D. Zhang, Z. Su, Q. He, Z. Wu, Y. Zhou, C. Pan, X. Liu and X. Feng, *J. Am. Chem. Soc.*, 2020, **142**, 15975–15985; (h) R. G. Biswas, S. K. Ray, V. K. Kannaujiya, R. A. Unhale and V. K. Singh, *Org. Biomol. Chem.*, 2021, **19**, 4685–4690; (i) S. J. Kalita, F. Cheng, Q.-H. Fan, N. Shibata and Y.-Y. Huang, *J. Org. Chem.*, 2021, **86**, 8695–8705; (j) I. N. C. Kiran, K. Fujita, K. Kobayashi, S. Tanaka and M. Kitamura, *Bull. Chem. Soc. Jpn.*, 2021, **94**, 295–308; (k) Y.-N. Li, X. Chang, Q. Xiong, X.-Q. Dong and C.-J. Wang, *Chin. Chem. Lett.*, 2021, **32**, 4029–4032; (l) P. Mahto, K. Shukla, A. Das and V. K. Singh, *Tetrahedron*, 2021, **87**, 132115; (m) V. A. Motornov, A. A. Tabolin, Y. V. Nelyubina, V. G. Nenajdenko and S. L. Ioffe, *Org. Biomol. Chem.*, 2021, **19**, 3413–3427; (n) Y. Suzuki, K. Kanemoto, A. Inoue, K. Imae and S.-i. Fukuzawa, *J. Org. Chem.*, 2021, **86**, 14586–14596; (o) H. Wang, C. Gong, C. Zhang, X. Zheng, Q. Hou, Q. Zhou,

- G. Zhou and Y. Chen, *Synlett*, 2021, **32**, 1437–1446; (p) O. Yildirim, M. Grigalunas, L. Brieger, C. Strohmann, A. P. Antonchick and H. Waldmann, *Angew. Chem., Int. Ed.*, 2021, **60**, 20012–20020; (q) G.-J. Wang, L. Wang, G.-D. Zhu, J. Zhou, H.-Y. Bai and S.-Y. Zhang, *Org. Lett.*, 2021, **23**, 8434–8438; (r) J. Corpas, A. Ponce, J. Adrio and J. C. Carretero, *Org. Lett.*, 2018, **20**, 3179–3182.
- 5 (a) K. Popandova-Yambolieva, *Collect. Czech. Chem. Commun.*, 1994, **59**, 489–494; (b) M. Maggini, G. Scorrano and M. Prato, *J. Am. Chem. Soc.*, 2002, **115**, 9798–9799; (c) B. C. Hong, A. K. Gupta, M. F. Wu, J. H. Liao and G. H. Lee, *Org. Lett.*, 2003, **5**, 1689–1692; (d) J. Jayashankaran, R. D. R. S. Manian and R. Raghunathan, *Tetrahedron Lett.*, 2004, **45**, 7303–7305; (e) R. D. R. S. Manian, J. Jayashankaran and R. Raghunathan, *Tetrahedron*, 2006, **62**, 12357–12362; (f) E. R. Zaitseva, A. Y. Smirnov, N. S. Baleeva and M. S. Baranov, *Chem. Heterocycl. Compd.*, 2019, **55**, 676–678.
- 6 (a) S. Filippone, E. E. Maroto, A. Martin-Domenech, M. Suarez and N. Martin, *Nat. Chem.*, 2009, **1**, 578–582; (b) E. E. Maroto, S. Filippone, A. Martin-Domenech, M. Suarez and N. Martin, *J. Am. Chem. Soc.*, 2012, **134**, 12936–12938; (c) E. E. Maroto, S. Filippone, M. Suarez, R. Martinez-Alvarez, A. de Cozar, F. P. Cossio and N. Martin, *J. Am. Chem. Soc.*, 2014, **136**, 705–712; (d) E. E. Maroto, J. Mateos, M. Garcia-Borras, S. Osuna, S. Filippone, M. A. Herranz, Y. Murata, M. Sola and N. Martin, *J. Am. Chem. Soc.*, 2015, **137**, 1190–1197.
- 7 (a) R. Taylor and D. R. M. Walton, *Nature*, 1993, **363**, 685–693; (b) F. Wudl, *Acc. Chem. Res.*, 2002, **25**, 157–161.
- 8 (a) M. Potowski, J. O. Bauer, C. Strohmann, A. P. Antonchick and H. Waldmann, *Angew. Chem., Int. Ed.*, 2012, **51**, 9512–9516; (b) M. Potowski, A. P. Antonchick and H. Waldmann, *Chem. Commun.*, 2013, **49**, 7800–7802.
- 9 Z. L. He, H. L. Teng and C. J. Wang, *Angew. Chem., Int. Ed.*, 2013, **52**, 2934–2938.
- 10 (a) M. J. S. Dewar, *Nature*, 1945, **155**, 50–51; (b) T. Nakajima and S. Katagiri, *Bull. Chem. Soc. Jpn.*, 1962, **35**, 910–916; (c) J. Griffiths and M. Lockwood, *J. Chem. Soc., Perkin Trans. 1*, 1976, 48–54.
- 11 For selected examples, see: (a) M. Diekmann, G. Bockstiegel, A. Lützen, M. Friedemann, W. Saak, D. Haase and R. Beckhaus, *Organometallics*, 2006, **25**, 339–348; (b) A. Cappelli, S. Galeazzi, I. Zanardi, V. Travagli, M. Anzini, R. Mendichi, S. Petralito, A. Memoli, E. Paccagnini, W. Peris, A. Giordani, F. Makovec, M. Fresta and S. Vomero, *J. Nanopart. Res.*, 2010, **12**, 895–903; (c) Y. Kosaka, K. Kitazawa, S. Inomata and T. Ishizone, *ACS Macro Lett.*, 2013, **2**, 164–167; (d) Y. Kosaka, S. Kawauchi, R. Goseki and T. Ishizone, *Macromolecules*, 2015, **48**, 4421–4430.
- 12 (a) B. S. Donslund, N. I. Jessen, J. B. Jakobsen, A. Monleon, R. P. Nielsen and K. A. Jørgensen, *Chem. Commun.*, 2016, **52**, 12474–12477; (b) B. S. Donslund, R. P. Nielsen, S. M. Monsted and K. A. Jørgensen, *Angew. Chem., Int. Ed.*, 2016, **55**, 11124–11128; (c) J.-F. Yue, G.-Y. Ran, X.-X. Yang, W. Du and Y.-C. Chen, *Org. Chem. Front.*, 2018, **5**, 2676–2679.
- 13 (a) M.-C. Tong, X. Chen, H.-Y. Tao and C.-J. Wang, *Angew. Chem., Int. Ed.*, 2013, **52**, 12377–12380; (b) Q.-H. Li, L. Wei and C.-J. Wang, *J. Am. Chem. Soc.*, 2014, **136**, 8685–8692; (c) H. L. Teng, L. Yao and C. J. Wang, *J. Am. Chem. Soc.*, 2014, **136**, 4075–4080; (d) X. Chang, X.-S. Sun, C. Che, Y.-Z. Hu, H.-Y. Tao and C.-J. Wang, *Org. Lett.*, 2019, **21**, 1191–1196; (e) C. Shen, Y. Yang, L. Wei, W.-W. Dong, L. W. Chung and C.-J. Wang, *iScience*, 2019, **11**, 146–159; (f) S.-M. Xu, L. Wei, C. Shen, L. Xiao, H.-Y. Tao and C.-J. Wang, *Nat. Commun.*, 2019, **10**, 5553; (g) X. Chang, Y. Yang, C. Shen, K.-S. Xue, Z.-F. Wang, H. Cong, H.-Y. Tao, L. W. Chung and C.-J. Wang, *J. Am. Chem. Soc.*, 2021, **143**, 3519–3535; (h) X. Chang, X. Cheng and C.-J. Wang, *Chem. Sci.*, 2022, **13**, 4041–4049; (i) C. S. Huachao Liu, Xin Chang, Chunjiang Wang, *Chin. J. Org. Chem.*, 2022, **42**, 3322–3334; (j) L. Xiao, B. Li, F. Xiao, C. Fu, L. Wei, Y. Dang, X.-Q. Dong and C.-J. Wang, *Chem. Sci.*, 2022, **13**, 4801–4812; (k) X. Xu, L. Bao, L. Ran, Z. Yang, D. Yan, C.-J. Wang and H. Teng, *Chem. Sci.*, 2022, **13**, 1398–1407.
- 14 (a) R. Misra, R. C. Pandey and J. V. Silverton, *J. Am. Chem. Soc.*, 1982, **104**, 4478–4479; (b) P. Jimonet, A. Boireau, M. Chevé, D. Damour, A. Genevois-Borella, A. Imperato, J. Pratt, J. C. R. Randle, Y. Ribeill, J.-M. Stutzmann and S. Mignani, *Bioorg. Med. Chem. Lett.*, 1999, **9**, 2921–2926; (c) P. de Almeida Leone, A. R. Carroll, L. Towerzey, G. King, B. M. McArdle, G. Kern, S. Fisher, J. N. A. Hooper and R. J. Quinn, *Org. Lett.*, 2008, **10**, 2585–2588; (d) A. C. Wei, M. A. Ali, Y. K. Yoon, R. Ismail, T. S. Choon, R. S. Kumar, N. Arumugam, A. I. Almansour and H. Osman, *Bioorg. Med. Chem. Lett.*, 2012, **22**, 4930–4933; (e) Y. Zheng, C. M. Tice and S. B. Singh, *Bioorg. Med. Chem. Lett.*, 2014, **24**, 3673–3682; (f) Y.-J. Zheng and C. M. Tice, *Expert Opin. Drug Discovery*, 2016, **11**, 831–834.
- 15 (a) C. J. Wang, G. Liang, Z. Y. Xue and F. Gao, *J. Am. Chem. Soc.*, 2008, **130**, 17250–17251; (b) Z.-Y. Xue, Q.-H. Li, H.-Y. Tao and C.-J. Wang, *J. Am. Chem. Soc.*, 2011, **133**, 11757–11765.
- 16 CCDC 2234947 ((1R,2'S,5'S)-3j), 2256257 (1R,3S,3aR,8aS,E)-4i contain the supplementary crystallographic data for this paper.
- 17 M. Hashimoto and S. Terashima, *Tetrahedron Lett.*, 1994, **35**, 9409–9412.
- 18 (a) See computational details in the ESI[†]; (b) Y.-h. Lam, M. N. Grayson, M. C. Holland, A. Simon and K. N. Houk, *Acc. Chem. Res.*, 2016, **49**, 750–762; (c) Q. Peng and R. S. Paton, *Acc. Chem. Res.*, 2016, **49**, 1042–1051; (d) R. B. Sunoj, *Acc. Chem. Res.*, 2016, **49**, 1019–1028; (e) D. J. Tantillo, *Acc. Chem. Res.*, 2016, **49**, 741–749; (f) X. Zhang, L. W. Chung and Y.-D. Wu, *Acc. Chem. Res.*, 2016, **49**, 1302–1310; (g) S. Ahn, M. Hong, M. Sundararajan, D. H. Ess and M.-H. Baik, *Chem. Rev.*, 2019, **119**, 6509–6560; (h) J. N. Harvey, F. Himoto, F. Maseras and L. Perrin, *ACS Catal.*, 2019, **9**, 6803–6813; (i) J. Lan, X. Li, Y. Yang, X. Zhang and L. W. Chung, *Acc. Chem. Res.*, 2022, **55**, 1109–1123.
- 19 Selected related computational studies: (a) D. H. Ess and K. N. Houk, *J. Am. Chem. Soc.*, 2008, **130**, 10187–10198; (b)

- M. Wang, C.-J. Wang and Z. Lin, *Organometallics*, 2012, **31**, 7870–7876; (c) A. Pascual-Escudero, A. de Cózar, F. P. Cossío, J. Adrio and J. C. Carretero, *Angew. Chem., Int. Ed.*, 2016, **55**, 15334–15338; (d) L. R. Domingo, M. Ríos-Gutiérrez and P. Pérez, *J. Org. Chem.*, 2018, **83**, 10959–10973; (e) F. Cheng, S. J. Kalita, Z.-N. Zhao, X. Yang, Y. Zhao, U. Schneider, N. Shibata and Y.-Y. Huang, *Angew. Chem., Int. Ed.*, 2019, **58**, 16637–16643; (f) Y. Xiong, Z. Du, H. Chen, Z. Yang, Q. Tan, C. Zhang, L. Zhu, Y. Lan and M. Zhang, *J. Am. Chem. Soc.*, 2019, **141**, 961–971; (g) S. V. Kumar and P. J. Guiry, *Angew. Chem., Int. Ed.*, 2022, **61**, e202205516; (h) B. Li, H. Xu, Y. Dang and K. N. Houk, *J. Am. Chem. Soc.*, 2022, **144**, 1971–1985.
- 20 Our computational studies on first-row transition-metal catalysis: (a) L. Xu, L. W. Chung and Y.-D. Wu, *ACS Catal.*, 2016, **6**, 483–493; (b) W. Gao, H. Lv, T. Zhang, Y. Yang, L. W. Chung, Y.-D. Wu and X. Zhang, *Chem. Sci.*, 2017, **8**, 6419–6422; (c) J. Lan, T. Liao, T. Zhang and L. W. Chung, *Inorg. Chem.*, 2017, **56**, 6809–6819; (d) X. Zhang and L. W. Chung, *Chem. Eur. J.*, 2017, **23**, 3623–3630; (e) S.-B. Wu, T. Zhang, L. W. Chung and Y.-D. Wu, *Org. Lett.*, 2019, **21**, 360–364; (f) Y. Yang, X. Zhang, L.-P. Zhong, J. Lan, X. Li, C.-C. Li and L. W. Chung, *Nat. Commun.*, 2020, **11**, 1850; (g) X. Du, Y. Xiao, Y. Yang, Y.-N. Duan, F. Li, Q. Hu, L. W. Chung, G.-Q. Chen and X. Zhang, *Angew. Chem., Int. Ed.*, 2021, **60**, 11384–11390; (h) J. Lan, T. Zhang, Y. Yang, X. Li and L. W. Chung, *Inorg. Chem.*, 2022, **61**, 18019–18032.
- 21 L. Falivene, Z. Cao, A. Petta, L. Serra, A. Poater, R. Oliva, V. Scarano and L. Cavallo, *Nat. Chem.*, 2019, **11**, 872–879.
- 22 F. M. Bickelhaupt and K. N. Houk, *Angew. Chem., Int. Ed.*, 2017, **56**, 10070–10086.